TORSION SENSOR MADE OF A SUPER STRUCTURE FIBER BRAGG GRATING EMBEDDED INTO POLYMER MATRIX OF AN AUTOMOBILE COMPOSITE MATERIAL MECHANICAL PART

Sorin MICLOS[1], Dan SAVASTRU[2], Roxana SAVASTRU[3], Florina-Gianina ELFARRA[4], and Ion LANCRANJAN[5]

Results obtained in simulation of a Superstructure Fiber Bragg Grating (SFBG) torsion sensor embedded into the polymer matrix of a fiber reinforced composite material are presented. The SFBG sensor simulation points to an improved smart composite or metallic parts design to be operated under torsion loads in various applications. Simulation consists of correlating the fiber deformation under applied mechanical loads with the modified FBG characteristic reflection spectrum considering the polarization mode variations. The torsion mechanical loads induced shifts in the characteristic reflection spectrum of Bragg wavelength and side bands are analyzed.

Keywords: SFBG sensor, torsion sensor, smart polymer composite material.

1. Introduction

The main purpose of the paper consists of presenting simulation results accomplished into the development of a simulation model of a Superstructure Fiber Bragg Grating (SFBG) sensor embedded into the polymer matrix of a composite material. The developed simulation model is dedicated to the study of torsion effects appeared into the composite material. In other words, SFBG is operated as a torsion sensor [1-10]. The main operation mode of the SFBG under twisting mechanical loads, i.e. as a torsion sensor, consists in observing the modification of reflection spectral response [11-17]. SFBG is a relatively new photonic device which has the constructive advantage of being easier to be intimately stuck into a metallic mount [11-17]. In this way the embedment into a polymer matrix of a composite material is facilitated. As previously mentioned,

[1] Eng., National Institute of R&D for Optoelectronics- INOE 2000, Romania, e-mail: miclos@inoe.ro
[2] Dr. Eng., National Institute of R&D for Optoelectronics- INOE 2000, Romania, e-mail: dsavas@inoe.ro
[3] Dr. Eng., National Institute of R&D for Optoelectronics- INOE 2000, Romania, e-mail: rsavas@inoe.ro
[4] Phys., "Saint John" Emergency Clinical Hospital, Romania e-mail: gianina.elfarra@gmail.com
[5] Phys., National Institute of R&D for Optoelectronics- INOE 2000, Romania, e-mail: ion.lancranjan@inoe.ro

the main purpose of the work is the improved design and development of devices based on optical fiber sensors, more specifically on the new type of optical Fiber Bragg Gratings (FBG) sensors [1-16], namely SFBG. FBG, an already classical optical device, is a type of optical fibers whose reflection spectral response is modified by writing a permanent interference pattern (Bragg Grating) into the core, the grating being affected by applied strain and temperature [1-4, 8, 9, 17-19]. As a result, it can be calibrated for the measurement of physical parameters manifesting themselves in the changes of strain or temperature. These unique features of optical fiber sensors such as FBGs have encouraged the widespread use of the sensor and the development of optical fiber-based sensing devices for structural health measurements, failure diagnostics, thermal measurements, pressure monitoring, etc. [15-20]. These features include light weight, small size, long-term durability, robustness to electromagnetic disturbances, and resistance to corrosion [1-16]. Despite the encouraging features, there are some limitations and challenges associated with FBGs and their applications. One of the challenges associated with FBGs is the coupling of the effects of strain and temperature in the optical response of the sensors which affects the reliability and accuracy of the measurements [11-23]. Another limitation of FBGs is the insensitivity to the refractive index of their ambient medium [1-10]. In liquids, the refractive index is a function of concentration. Making FBGs sensitive to the ambient refractive index and keeping their thermal sensitivity intact enables optical sensors with the capability of the simultaneous measurement of concentration and temperature in liquids or of strain and temperature in the case of structural monitoring. Considering the unique features of FBGs, embedding the sensors in metal parts for in-situ load monitoring is a cutting-edge research topic. Several industries such as machining tools, aerospace, and automotive industries can benefit from this technology [5-23]. The metal embedding process is a challenging task, as the thermal decay of UV-written Bragg gratings can starts at a temperature of ~200 ˚C and accelerates at higher temperatures [5-23]. As a result, the embedding process needs to be performed at low temperatures [11-23]. To properly design the sensing devices and analyze the performance of the sensors, an optomechanical model of FBGs for thermal and structural monitoring is necessary. The model is derived from the photo-elastic and thermo-optic properties of optical fibers. The developed model can be applied to predict the optical responses of a FBG exposed to structural loads and temperature variations with uniform and non-uniform distributions [2-4]. The model is also extended to obtain optical responses of superstructure FBGs in which a secondary periodicity is induced in the index of refraction along the optical fiber. The secondary periodicity along the optical fiber of its core refraction index can be induced by metallic thin film deposition on optical fiber outer surface, creating in this way a Superstructure FBG [5-23].

To address the temperature-strain coupling in FBGs, SFBG with on-fiber metal thin films are designed and manufactured. It is shown that SFBGs have the capability of measuring strain and temperature simultaneously. The design of the sensor with on-fiber thin films is performed by using the developed optic-mechanical model of FBGs. This paper presents the results obtained in simulation of the SFBGs optomechanical sub-model developed specially for evaluation and design of a torque sensor to be used as embedded in mechanical parts with cylindrical shape.

2. Theory

In Fig. 1 and 2 there are schematically presented the investigated SFBG and the optic fiber torsion mechanism. Fiber twisting occurs very often but has almost no influence on usual applications of the SMF for optical pulse signal transportation. However, twists certainly cause changes in the polarization state of the propagating light wave, which are important in some situations [13]. The twisted fiber is regarded as a twisted elastic rod with its axis kept straight, as shown in Fig. 1. The torsion is characterized by the twist rate, namely twisted angle per unit length of fiber.

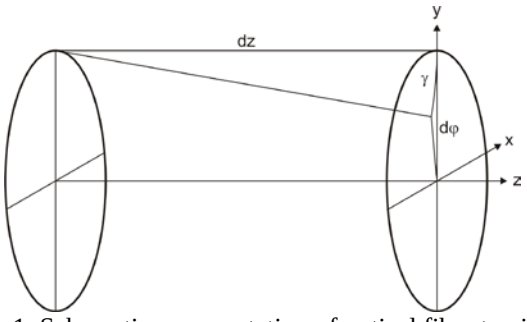

Fig. 1. Schematic representation of optical fiber torsion.

In Fig. 2 there is schematically presented the coordinate systems which are used and interchanged for development of the system of mathematical equations on which the developed simulation model is based.

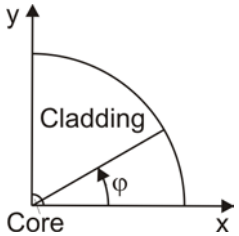

Fig. 2. Coordinate system used in simulation model.

This simulation model is rigorous even complicated and represents with good accuracy experimental results on bending and torsion of fibers, allows analyses on torsion-induced biaxial refraction properties and on polarization state evolution in twisted optic fibers based on coupled mode theory (CMT).

The key parameter to be observed when investigating the SFBG and FBG sensing devices is λ_B, the Bragg wavelength, defined as

$$\lambda_B = 2n_{eff} \cdot \Lambda \tag{1}$$

where Λ is the grating pitch length. n_{eff} is the effective value of the optical fiber core refractive index which is obtained after some algebra and satisfy the condition

$$n_{clad} < n_{eff} < n_{core} \tag{2}$$

where n_{clad} is the refractive index of the cladding and n_{core} is the refractive index of the core [11-17]. The Bragg wavelength is the peak of the FBG characteristic reflection band [11-17]. The SFBG and FBG mode of operation consists mainly of observing the spectral shift of the Bragg wavelength and of the spectral broadening of the Bragg reflection band and of its possible reduction [11-17]. Consequently, the simulation model of the SFBG and/or FBG sensing device can be constructed rigorously based on coupled mode theory (CMT) [11-17].

There is an alternative to the previously mentioned simulation model [11-17]. The alternative model is rather a phenomenological one theoretical basis of the SFBG sensor investigation consists of: (1) definition of the FBG and SFBG reflectivity dependence on the induced mechanical strain by the core refractive index variation and (2) definition of the relationship between the applied torque T and the torsional stress τ in the SFBG. Basically, a FBG or a SFBG sensor, with a sub-micron periodic modulation of the core index of refraction, functions as a filter. When a Bragg grating is exposed to a broadband spectrum of light, the guided light wave, propagating along the optical fiber, is scattered by each grating plane. As a result, parts of the spectrum at specific wavelengths are reflected. The coupling between the forward and backward propagating modes results in a resonance condition. The resonance occurs at a specific wavelength called the Bragg wavelength (λ_B). Wavelengths not coincident with the Bragg condition degenerate progressively with weak reflections, whereas wavelengths close to the resonance wavelength determined by the Bragg condition undergo strong reflections. The Bragg wavelength is related to the effective propagating mode index of refraction, neff, and the grating parameters, as defined in the Bragg condition [11, 14].

3. Simulation results

The simulation results were accomplished considering that the SFBG and/or FBG is manufactured into a SM optical fiber considered as standard,

namely Fibercore SM750 type optical fiber, which is, according to literature, commonly used as host for FBG [11-17]. For short, this means that the optical fiber core has a diameter of 2.8 up to 3.5 μm and a refractive index of 1.4585, its cladding has a 62.5 μm diameter with a refractive index of 1.4540 [11-17]. The grating FBG was considered as the number of pitches N in the range 1000 - 20000 and a length in the range 1 - 15 mm. The first step in performing the SFBG and of FBG simulation consists in defining the effective value of SM optical fiber refractive index in Eq. (1). The next step consists of guessing a possible Bragg wavelength, the so-called "design wavelength".

In this moment, a relatively delicate issue must be solved. The investigated SFBG and/or FBG is embedded in the polymer matrix of a composite material adhering to it. In the SFBG case, the grating created by periodic metallic thin layer represent also an intermediate mechanical mount. The polymer matrix is considered as a mechanical mount of the optical fiber on which a torque is applied. Because it must be a torque sensor, meaning rotation as an effect of applying a torque upon a mount will be the main process to be watched, this polymer mechanical mount should be preferably of cylindrical shape, with the SFBG or FBG sensor placed on its axis. The simulations were performed considering that the SFBG or FBG sensor is firmly stacked along the axis of a polymer shaft. The consequent classical problem of mechanics appears like this: if torque T is applied to the shaft, as it will twist about its axis, what will be the shear stress upon the optical fiber cladding outer surface? Certain assumptions are considered as necessary for the simulations: the circular polymer shaft has an uniform cross section; a cross section perpendicular to the axis is made at a certain point in the shaft, it will remain plane and perpendicular after the torque is applied; the diameter of the polymer shaft stays constant; a radial line on the section would remain radial after torque T is applied; cross sections perpendicular to the axis rotate with respect to each other but remain plane and parallel; this rotation is the only deformation of the shaft; the elongation of the shaft is negligibly small [7-15]. After some algebra applying the Hooke's Law, a linear relationship between the torque T applied on the outer shaft surface and the torsional stress τ in the shaft is derived [7-15]. For the performed simulations, the length of the polymer shaft, L, was 1 mm. Simulations were performed considering a 25 mm diameter circular polymer shaft and the optical fiber fused silica having a Young's modulus $E = 2 \cdot 10^{11}$ N/m^2, and the modulus of elasticity of shear G = 80 GPa. It is worth to notice an important assumption made in performing the simulation of SFBG or FBG embedded into polymer matrix torque sensor, namely that the applied torque on the outer optical fiber cladding surface can be approximated as it is on the external surface of a polymer layer of 1 - 5 μm which makes a common body with the embedded optic fiber [11-15]. This

approximation is an empirical one based on experimental observation which is considered as valid for applied forces up to 10 kN [11-15].

The SFBG or FBG simulation next step consists of describing as accurate as possible the spectrum of the FBG reflectivity. The simulation was performed by solving the differential equation which describes reflection spectrum ρ (λ) of a given SFBG or FBG as a function of λ with *z*, the displacement along the optical axes, as a parameter. The investigated SFBG or FBG have accurate defined mechanical parameters such as Young modulus, *E*, and Poisson number, *v*. The copper metallic thin film deposited on optical fiber outer surface of SFBG was considered as continuous with 0.25 μm thickness. The term base photosensitive optical fiber means that a Bragg grating will be written over at least 1 mm length. The Bragg grating, as the main component of the SFBG or FBG sensor is investigated as placed inside the polymer shaft with which is a common body. The applied force on the outer surface of the polymer shaft was considered to vary in the range 1 N - 2500 N. The torque is considered as having a constant arm of 12.5 mm. For calculating the effective torque applied on optic fiber, there was considered an arm of the 75 μm.

In Fig. 3 and 4 there are presented the simulated results accomplished in evaluating the effective value of optical fiber core refractive index, n_{effco}, (Fig. 3) and normalized frequency *V* (Fig. 4) as functions of light wavelength.

In Fig. 5 there is presented the curve used for evaluation of applied stress/torsion using the previously defined approximation. In all the investigated cases the stress/torque arm was of 75 μm (including the optical fiber radius).

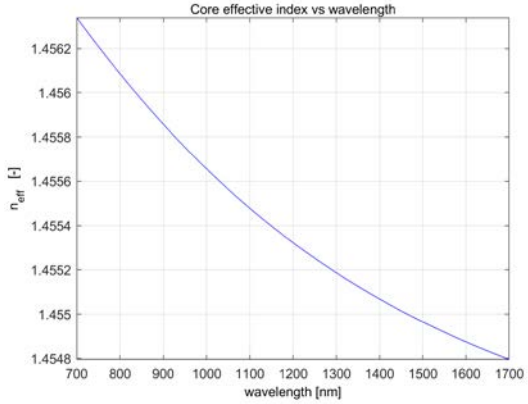

Fig. 3. Simulated variation of core refractive index effective value vs incident light wavelength.

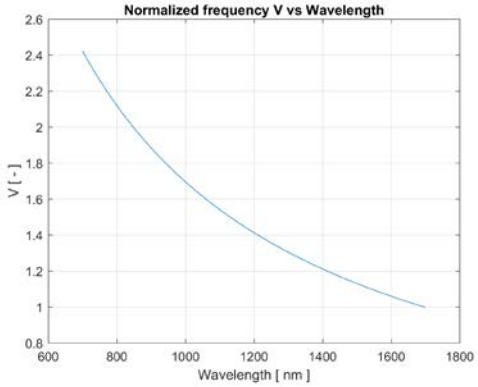

Fig. 4. Simulated variation of normalized frequency V vs incident light wavelength.

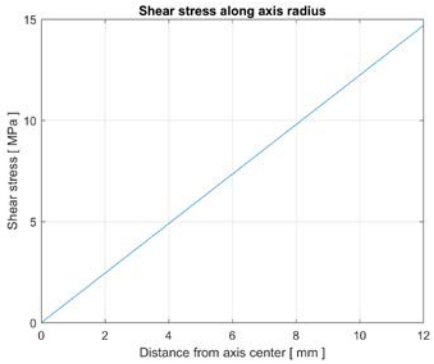

Fig. 5. Calculated shear stress applied on the optical fiber vs distance from the polymer shaft axis.

In Fig. 6 is presented the shift of the Bragg grating reflection spectra simulated in the case of a FBG of 10 mm length with N = 10000 pitches at a torque/stress of ~250 Nm (a force of ~1000 N applied on the outer polymer shaft surface). In Fig. 7 is presented the shift of the Bragg grating reflection spectra simulated in the case of an FBG of 5 mm length with N = 2500 pitches at a torque/stress of ~550 Nm (a force of ~1250 N applied on the outer polymer shaft surface).

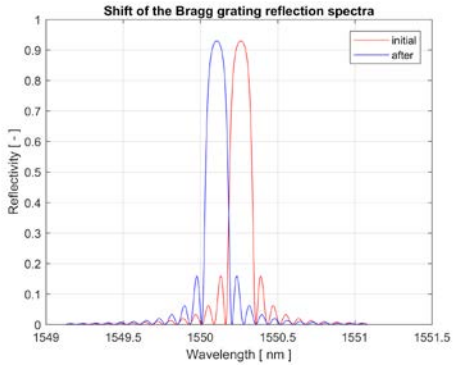

Fig. 6. Shift of the Bragg grating reflection spectra simulated in the case of an FBG of 10 mm length with 1000 N applied force (red - initial; blue - after applied torsion).

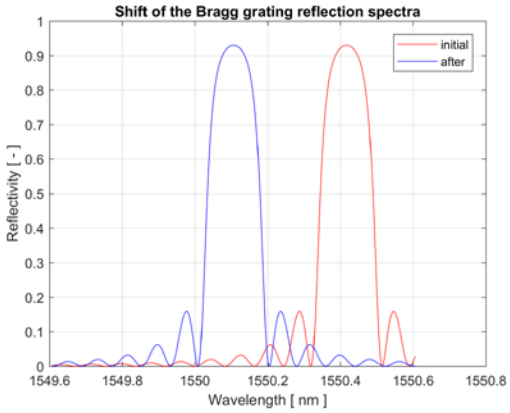

Fig. 7. Shift of the Bragg grating reflection spectra simulated in the case of an FBG of 5 mm length with an applied force of 1250 N (red - initial; blue - after applied torsion).

In Fig. 8 is presented the shift of the Bragg grating reflection spectra simulated in the case of an FBG of 5 mm length with N = 2500 pitches at a torque/stress of ~275 Nm (a force of ~625 N applied on the outer polymer shaft surface). In Fig. 9 is presented the shift of the Bragg grating reflection spectra simulated in the case of an FBG of 10 mm length with N = 10000 pitches at a torque/stress of ~75 Nm (a force of ~225 N applied on the outer polymer shaft surface).

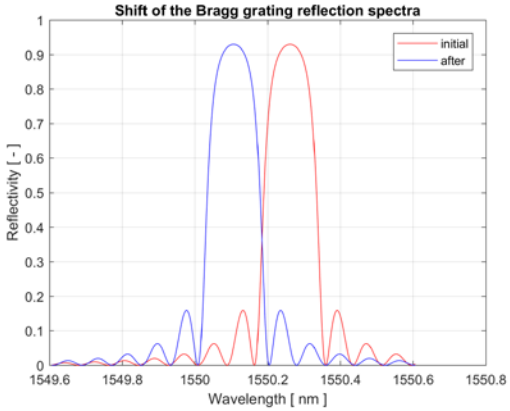

Fig. 8. Shift of the Bragg grating reflection spectra simulated in the case of an FBG of 5 mm length with an applied force of ~625 N (red - initial; blue - after applied torsion). (red - initial; blue - after applied torsion).

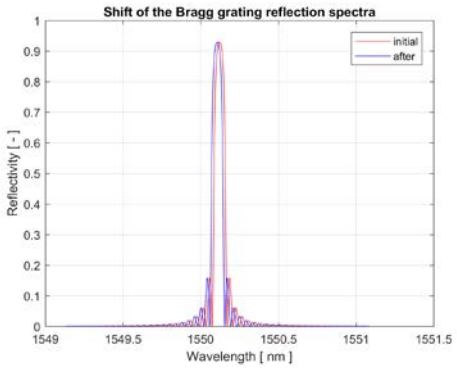

Fig. 9. Shift of the Bragg grating reflection spectra simulated in the case of a FBG of 10 mm length with an applied force of ~225 N (red - initial; blue - after applied torsion).

Regarding the results presented in Figs. 5, 6, 7, 8 and 9 it is worth to mention that the SFBG sensor, an optical fiber, must be mounted into some mechanical intermediate part. Because it must be a torque sensor, meaning rotation as an effect of applying a torque upon a mount will be the main process to be watched, this mechanical mount should be preferably of cylindrical shape, with the SFBG sensor placed on its axis. The simulations were performed considering that the SFBG sensor is firmly stacked along the axis of a metallic shaft.

The consequent classical problem of mechanics appears like this: if torque T is applied to the shaft, as it will twist about its axis, what will be the shear stress upon the fiber optic outer surface? Certain assumptions are considered as necessary for the simulations: the circular shaft has an uniform cross section; a cross section perpendicular to the axis is made at a certain point in the shaft, it will remain plane and perpendicular after the torque is applied; the diameter of the shaft stays constant; a radial line on the section would remain radial after torque T is applied; cross sections perpendicular to the axis rotate with respect to each other but remain plane and parallel; this rotation is the only deformation of the shaft; the elongation of the shaft is negligibly small. After some algebra applying the Hooke's Law, a linear relationship between the torque T applied on the outer shaft surface and the torsional stress τ in the shaft is derived.

For the performed simulations, the length of the shaft, L, was 1 mm. Simulations were performed considering a 1-inch diameter circular shaft, having a Young's modulus $E = 2 \cdot 10^{11}$ N/m^2, and modulus of elasticity of shear $G = 80$ GPa. Describing as accurate as possible the spectrum of the FBG reflectivity. The simulation was performed by solving the differential equation which describes reflection spectrum $\rho(\lambda)$ of a given SFBG as a function of λ with z, displacement along the optic axes, as a parameter. The studied SFBGs have accurate defined mechanical parameters such as Young modulus, E, and Poisson number, v. The copper metallic thin film deposited on optic fiber outer surface was considered as continuous with 0.25 μm thickness.

The second step of the second stage of the simulation is most laborious. It is the main part of the simulation. Using the data obtained from solving the mechanical problem of Stage 1, namely the shear at the surface of the optical fiber, the shift of the Bragg grating peak is calculated. A dedicated software which was used to calculate the Bragg grating reflection peak shift admits, as inputs, the shaft diameter and length values, the base fiber optic glass and shaft material Young's modulus and modulus of elasticity of shear, the Bragg grating parameters, namely, its length, its number of pitches.

This software was developed to obtain an improved design of a torque SFBG sensor by optimizing mechanical mount parameters and Bragg grating specification. It is important to mention that Stage 2 was realized considering the three layers optical fiber model. In the followings, some examples of the results are presented. The values of applied torque, shaft diameter and length, number of Bragg grating pitches are mentioned in each case. The results were calculated for the basic, the standard configuration. The simulation was performed considering the defined configuration of the optical fiber. It can be observed that the reflectivity spectra characteristics could be unappropriated for torque measuring applications.

The lengthening of the shaft, implicitly of the Bragg grating one, appears as a design solution for improving the torque SFBG sensor characteristics. However, lengthening of shaft length has therefore more technological difficulties in stacking the optic fiber into the shat. Increasing the Bragg grating pitches has as a result, the increase of its reflectivity and of its peak shift discrimination capability. The calculated Bragg grating peak shifts presented in Fig. 6 and 7 were obtained considering the described configuration. The calculated Bragg grating peak shifts were of 195.58 pm in Fig. 7, of 309.56 pm in Fig. 9, 215.25 pm in Fig. 6 and of 85.25 pm in Fig. 7. In Fig. 8, the results obtained in the case of a slightly modified new configuration are presented. The applied momentum was of 100 Nm, the Bragg grating length was of 10 mm and its number of pitches was 10000. A Bragg grating peak shift of 65.79 pm was calculated.

There were performed simulations considering a circular shaft made of a copper alloy, having a Young's modulus $E = 2 \cdot 10^{11}$ N/m^2, a modulus of elasticity of shear G = 83 GPa. The shear at of the optic fiber with a torque of 100 Nm applied upon the shaft surface was calculated as 255 kPa, as 572 kPa for 200 Nm, as 47 kPa for 10 Nm.

4. Conclusions

For a given commercial optical fiber, the results obtained in calculations of core and clad effective refractive indexes variations over an extended propagation wavelength range as a starting point of the embedded in polymer FBG and/or SFBG torsion effects simulation are presented. The SFBG sensor simulation provided useful results for torsion sensors design. The influence of SFBG

parameters was studied. Applying the same stress (100 Nm) on fibers of same core diameter (5 μm) but of different Bragg grating lengths (1 and 10 mm) the peak shift increases from 195.58 pm to 309.56 pm. The longer is the grating the more sensitive is the sensor. For different fibers (3.5 and 5 μm) of same grating length (10 mm) and subjected to the same stress (100 Nm) the peak shift increases from 65.79 pm to 309.56 pm. A larger core diameter improves sensitivity. These are some examples from the study.

The simulation was performed for four commercially available photosensitive single mode silica optical fibers having different geometric and optical characteristics, mainly core and cladding refractive index values. The simulation results are in good agreement with the experimental ones reported in literature [12-14].

The results obtained in calculation of coupling coefficients of core and cladding radiation modes, followed by the ones obtained in evaluation of absorption coefficients are presented as the simulation next stages.

The final two stages, the transmission spectra, the shift and the bandwidth broadening specific for a resonant wavelength, both induced by a bending deformation of optic fiber, are presented as calculated by using the developed software design package.

In subsidiary, the presented results are part of a software design package dedicated to optimization of long period grating parameters, overall length and period, which are to be manufactured into a given single mode fiber with the environment parameters to be measured with the resulting optical fiber sensor.

In this sense, the software design package proves to be useful for calculation of core and cladding refractive index variations with propagation wavelength, long period grating resonance wavelengths as depending on its period, the absorption coefficients at these resonance wavelengths and consequently, of its transmission spectra.

The above mentioned long period grating software design package is under current development, the immediate improvement will consist in using the three layers optical fiber model and in increasing the number of cladding propagation modes used in calculations.

This research is supported by MANUNET grant MNET17/ NMCS0042 and by the Core Program project no. PN 18 28.01.01.

R E F E R E N C E S

[1]. *K. T. Lau, C. C. Chan, L. M. Zhou, W. Jin*, "Strain monitoring in composite-strengthened concrete structures using optical fibre sensors", in Compos Part B-Eng, **vol**. **32**, no. 1, 2001, 33-45.

[2]. *T. Vella, S. Chadderdon, R. Selfridge, S. Schultz, S. Webb, et al.*, "Full-spectrum interrogation of fiber Bragg gratings at 100 kHz for detection of impact loading", in Meas Sci Technol, **vol**. **21**, no. 9, 2010, 094009.

[3]. *A. Propst, K. Peters, M. A. Zikry, W. Kunzler, Z. Zhu, et al.*, "Dynamic, full-spectral interrogation of fiber Bragg grating sensors for impact testing of composite laminates", in Proc SPIE, **vol. 7503,** 75030G-1, 2009.
[4]. *B. Van Hoe, E. Bosman, J. Missinne, S. Kalathimekkad, G. Lee, et al.*, "Low-cost fully integrated fiber Bragg grating interrogation system", in Proc SPIE, **vol. 8351,** 83510U–1, 2012.
[5]. *F. Berghmans*, Optical Sensor Course, Vrije Universiteit Brussel, Brussels, 2015.
[6]. *A. Othonos*, Bragg Gratings in Optical Fibers: Fundamentals and Applications. In *K. T. V. Grattan, B. T. Meggitt* eds. Optical Fiber Sensor Technology, Springer, New York, 2000.
[7]. *V. Karbhari, V. M. Karbhari*, Health monitoring, damage prognosis and service-life prediction - Issues related to implementation. In *Farhad Ansari* ed. Sensing Issues in Civil Structural Health Monitoring, Springer, Dordrecht, 2005.
[8]. *T. Geernaert, S. Sulejmani, C. Sonnenfeld, K. Chah, G. Luyckx, et al.*, "Internal strain monitoring in composite materials with embedded photonic crystal fiber Bragg gratings", in Proc SPIE, **vol. 9226**, 92260D, 2014.
[9]. *D. Savastru, S. Miclos, R. Savastru, I. Lancranjan*, "Numerical Analysis of a Smart Composite Material Mechanical Component Using an Embedded Long Period Grating Fiber Sensor", in Proc SPIE, **vol. 9517**, 95172A, 2015.
[10]. *S. Miclos, D. Savastru, R. Savastru, I. Lancranjan*, "Numerical analysis of Long Period Grating Fibre Sensor operational characteristics as embedded in polymer", in Compos Struct, vol. **183**, no. SI, 2018, pp. 521-526.
[11]. *D. Savastru, S. Miclos, R. Savastru, I. Lancranjan*, "Study of thermo-mechanical characteristics of polymer composite materials with embedded optical fibre", in Compos Struct, vol. **183**, no. SI, 2018, pp. 682-687.
[12]. *K. S. Kim, Y. Ismail, G. S. Springer*, "Measurements of Strain and Temperature with Embedded Intrinsic Fabry-Perot Optical Fiber Sensors", in J Compos Mater, **vol. 27**, 17, Dec. 1993, pp. 1663-1677.
[13]. *L. Weisenbach*, Fiber optic sensors, BCC Research, Tech. Rep. IAS002D, 2008.
[14]. *L. Thevenaz*, Advanced Fiber Optics: Concepts and Technology, EPFL Press, Lausanne, 2011.
[15]. *S. Miclos, D. Savastru, I. Lancranjan*, "Numerical Simulation of a Fiber Laser Bending Sensitivity", in Rom Rep Phys, **vol. 62**, no. 3, 2010, pp. 519-527.
[16]. *S. Miclos, D. Savastru, I. Lancranjan*, "Numerical analysis of an active FBG sensor", in Procs. ACS, Malta, 2010, pp. 490-497.
[17]. *D. Savastru, S. Miclos, I. Lancranjan*, "Theoretical analysis of an active FBG sensor output noise", in Procs. ACS, Malta, 2010, pp. 498-503.
[18]. *I. Lancranjan, S. Miclos, D. Savastru*, "Numerical simulation of a DFB-fiber laser sensor (I)", in J Optoelectron Adv M, **vol. 12**, no. 8, Aug. 2010, pp. 1636-1645.
[19]. *K. S. C. Kuang, W. J. Cantwell*, "Use of conventional optical fibers and fiber Bragg gratings for damage detection in advanced composite structures: A review", in Appl Mech Rev, **vol. 56**, no. 5, 2003, pp. 493-513.
[20]. *I. Lancranjan, S. Miclos, D. Savastru, A. Popescu*, "Numerical simulation of a DFB-fiber laser sensor (II) - theoretical analysis of an acoustic sensor", in J Optoelectron Adv M, **vol. 12**, no. 12, Dec. 2010, pp. 2456-2461.
[21]. *R. Savastru, I. Lancranjan, D. Savastru, S. Miclos*, "Numerical simulation of distributed feed-back fiber laser sensors", in Proc SPIE, **vol. 8882**, 88820Y, 2013.
[22]. *S. Miclos, D. Savastru, R. Savastru, I. Lancranjan*, "Design of a Smart Superstructure FBG Torsion Sensor", in Proc SPIE, vol. **9517**, 95172B, 2015.
[23]. *D. Savastru, S. Miclos, R. Savastru, I. Lancranjan*, "Analysis of optical microfiber thermal processes", in Rom Rep Phys, **vol. 67**, no. 4, 2015, pp. 1586-1596.